Numerical Evidence of Fast Dynamo Action in a Spherical Shell

R. Hollerbach
Institute of Geophysics and Planetary Physics, Los Alamos National Laboratory, Los Alamos, New Mexico 87545

D. J. Galloway
School of Mathematics and Statistics, University of Sydney, Sydney, New South Wales 2006, Australia

M. R. E. Proctor
Department of Applied Mathematics and Theoretical Physics, University of Cambridge, Cambridge, CB3 9EW, United Kingdom
(Received 18 August 1994)

We consider the evolution of a magnetic field in a spherical shell of highly conducting fluid surrounded by an insulator. We impose an axisymmetric, time-dependent flow, having large regions of chaotic particle paths. This flow appears to yield fast dynamo action, in which the field grows on the fast advective, rather than on the slow diffusive time scale. We demonstrate that the field adjusts to the Bondi-Gold theorem, according to which the field in the insulators inside and outside the shell cannot grow on the fast time scale, by becoming increasingly self-contained within the shell.

PACS numbers: 47.65.+a, 47.11.+j, 47.52.+j

The Sun's magnetic field is created by the dynamo action of fluid motions in the electrically conducting plasma [1–3], and the field is observed to evolve on the advective time scale. The natural time scale of dynamo action, however, is the diffusive time scale, 10^6 times longer in the case of the Sun. It is thus of interest to explore the possibility of dynamo action on the advective time scale—so-called fast dynamo action [4,5]. In this work we apply the ideas developed in a previous, plane-periodic model [6] to a spherical shell model and present numerical evidence of fast dynamo action for diffusive time scales up to 100 000 times longer than the advective time scale. It is of particular interest to consider fast dynamo action in a bounded domain such as a spherical shell, in view of the Bondi-Gold theorem [7], stating that the field in the insulators inside and outside the spherical shell cannot be amplified on the fast advective time scale. We consider the structure of the field and demonstrate that as the magnetic Reynolds number measuring the ratio of the time scales is increased, the structure becomes increasingly fine, and increasingly contained within the spherical shell.

The equation governing all dynamo action, slow and fast, is the induction equation for the magnetic field $\mathbf{B}$:

$$\frac{\partial}{\partial t}\mathbf{B} = \nabla \times (\mathbf{u} \times \mathbf{B}) + R_m^{-1}\nabla^2\mathbf{B},$$

here nondimensionalized in such a way that the advective time scale is order 1, and the diffusive time scale is order R_m. For the kinematic problem considered here, the fluid flow $\mathbf{u}$ is prescribed. The distinction between a slow and a fast dynamo then lies in the behavior of the growth rate of $\mathbf{B}$ as the magnetic Reynolds number R_m tends to infinity: If the growth rate tends to zero the dynamo is slow, whereas if it tends to some nonzero value the dynamo is fast. In other words, a slow dynamo does not amplify the field on the advective time scale, whereas a fast dynamo does.

It has been demonstrated [8,9] that in order to yield a fast dynamo, the flow $\mathbf{u}$ must have chaotic particle paths. This is readily understandable in terms of the frozen flux theorem, according to which in the limit $R_m \to \infty$ the fluid flow will tend to advect the field as if it were a material line, frozen into the fluid. Since chaotic flows are very efficient at stretching material lines, they are thus also very efficient at stretching and thereby amplifying magnetic field lines, although one must be sure that the folding which inevitably follows the stretching is constructive [10,11]. Chaotic flows are unfortunately not very amenable to analytic solutions. For this reason, much work in fast dynamo theory has focused on various related problems. For example, flows having singularities in the velocity [12] and in the vorticity [13] have been considered, but unfortunately the resulting fast dynamo action seems to depend crucially on these singularities. The exactly diffusionless limit $R_m \equiv \infty$ has also been considered [14], but again there is no formal proof that the limit $R_m \equiv \infty$ is the same as $R_m \to \infty$. Finally, models with a stochastic diffusion term have been considered [15].

In this work we present a direct numerical solution of the induction equation, with the proper diffusion term explicitly included. Growing solutions are sought in a spherical shell lying between $r_i = \frac{1}{2}$ and $r_o = \frac{3}{2}$, with the regions $r < r_i$ and $r > r_o$ taken to be source-free insulators. For the flow $\mathbf{u}$ we take

$$\mathbf{u} = \nabla \times [r^{-1} f(r,t) \sin\theta \cos\theta \,\hat{\mathbf{e}}_\phi] + r\,\omega(r,t) \sin\theta \,\hat{\mathbf{e}}_\phi .$$

As in the previous model [6] which forms the basis of this work, taking $\mathbf{u}$ to be axisymmetric enables us to focus separately on different azimuthal modes $\exp(im\phi)$ of the field $\mathbf{B}$. Cowling's theorem [16] disallows only the possibility of an axisymmetric flow generating an axisymmetric field. Only $m = 0$ is thus excluded *a priori.* For an axisymmetric flow to have chaotic particle paths, it must be time dependent. We thus take

$$f(r,t) = (r - \tfrac{1}{2})(r - \tfrac{3}{2})/2\sin[4\pi r + \sin(\pi/4t)],$$
$$\omega(r,t) = 2\sin[4\pi r + \sin(\pi/4t)].$$

The parabolic envelope $(r - \frac{1}{2})(r - \frac{3}{2})$ in f enforces the appropriate boundary condition of no normal flow at the inner and outer boundaries of the spherical shell. The $\sin[4\pi r + \sin(\pi/4t)]$ term then represents four circulation cells, as shown in Fig. 1(a), with the $\sin(\pi/4t)$ time dependent shaking them back and forth in r, with a period $T = 8$. As shown in Fig. 1(b), this flow has a very large region of chaotic particle paths.

For this particular equatorial symmetry of the flow, the field separates into distinct dipolar and quadrupolar symmetries. Thus, having decomposed the field as

$$\mathbf{B} = \nabla \times (g\hat{\mathbf{r}}) + \nabla \times \nabla \times (h\hat{\mathbf{r}}),$$

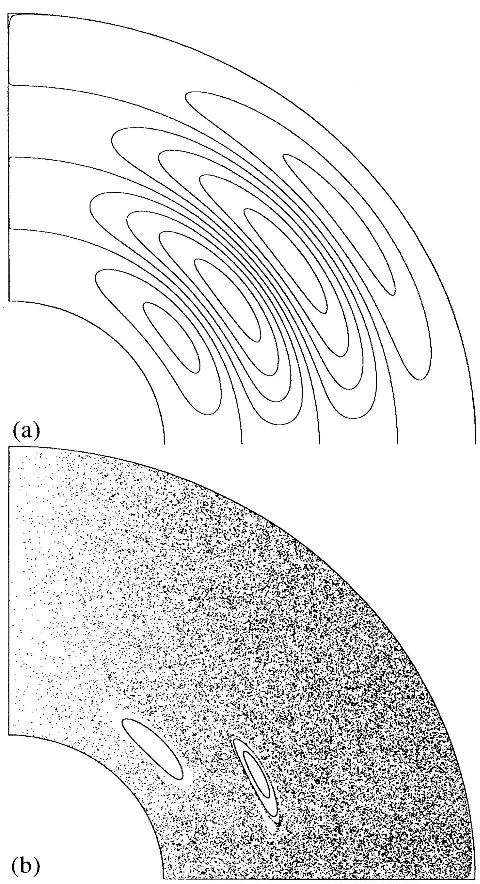

FIG. 1. (a) Instantaneous streamlines, at $t = 0$ modulo T, of the flow $\mathbf{u}_m = \nabla \times [r^{-1}f(r,t)\sin\theta\cos\theta\,\hat{\mathbf{e}}_\phi]$ in the meridional plane. (b) Poincaré section of the flow $\mathbf{u}_m$. Points are plotted at $t = 0$ modulo T.

we then expand g and h as

$$g = \sum_{n=1}^{N} g_n(r)P_{n_2}^m(\cos\theta)\exp(im\phi),$$
$$h = \sum_{n=1}^{N} h_n(r)P_{n_1}^m(\cos\theta)\exp(im\phi),$$

where for the dipolar symmetry $n_1 = 2n + m - 1, n_2 = 2n + m - 2$. Because of the particularly simple angular structure of the flow, the angular modes then couple only to adjacent models, that is, g_n couples only to itself, $g_{n\pm1}, h_{n-1}$, and h_n, and similarly h_n couples only to itself, $h_{n\pm1}, g_n$, and g_{n+1}. If we then finite difference $g_n(r)$ and $h_n(r)$, the radial grid points will also couple only to adjacent grid points. One can thus run the code reasonably efficiently even at very high truncations. It has been shown [17] that the field will exhibit structures as fine as $R_m^{-1/2}$, as a result of a simple balance between advection and diffusion within these fine structures. For $R_m = 10^5$ one should thus expect structures as fine as $O(1/300)$. The largest truncation used in this work is $N = 512$ angular modes times 1000 radial grid points and appears to be sufficient to resolve these structures. Finally, to test the code, at low R_m, and thus low truncations, one can benchmark it against a more general, but consequently less efficient code [18].

Starting the code with a random (divergence-free) initial field, it was found that after a dozen or so flow periods T the eigensolutions had established themselves, and thereafter the entire solution grew by the same factor over each successive period T. The average growth rate over a period is shown in Fig. 2, for the dipolar $m = 1$ mode. It is *very* well fit by the curve $0.21 - 0.12(1000/R_m)^{1/2}$, which would suggest that for large R_m it levels off to 0.21. (For comparison, the largest Lyapunov exponent is about 0.15.) The increase in the growth rates between $R_m = 40\,000$ and $100\,000$ is less than 4%. It is this leveling off of the growth rate that provides evidence of fast dynamo action. It must be emphasized, though, that this numerical evidence is not proof; it is conceivable that for even larger R_m the growth rate would decrease to zero again. By their very nature, numerical solutions will always fall somewhat short of infinity. Nevertheless, in view of this smooth leveling off, it seems likely that this behavior will continue for even larger R_m.

It is curious, though, that one must go to $R_m \approx 10^5$ before the growth rate levels off; in the previous plane-periodic model [6] the growth rates leveled off at $R_m \approx 10^2$ to 10^3. We believe the reason may be the following: In this spherical model the azimuthal wave number m is restricted to integer values, whereas in the plane-periodic model the corresponding wave number k is unrestricted. The extra freedom of being able to optimize k may explain why the growth rates leveled off sooner in

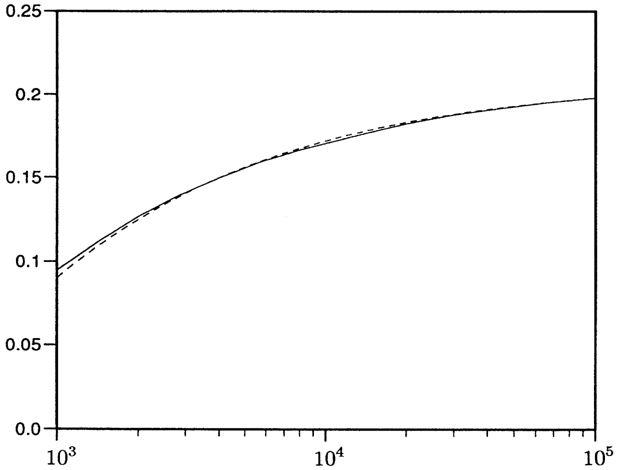

FIG. 2. The solid line shows the growth rate of the dipolar $m = 1$ mode, plotted against R_m on a logarithmic scale. The dashed line shows the curve $0.21 - 0.12(1000/R_m)^{1/2}$.

the plane-periodic model. Indeed, for most other values of k it did not level off so soon [19].

Figure 3 shows the structure of the eigensolutions at $t = 0$ modulo T for $R_m = 10\,000$ on the left and 40 000 on the right. One notes first that the field is closely aligned with the instantaneous streamlines of the flow at $t = 0$, shown in Fig. 1(a). As in the plane-periodic case, it appears to accumulate at the stagnation points and is then drawn out from there. In both the plane-periodic and spherical cases, the field generation appears to arise because of heteroclinic tangling between the stagnation points. As expected [17], the field exhibits structure on a very fine scale, consistent with an $R_m^{-1/2}$ scaling. In the limit $R_m \to \infty$ these eigensolutions then tend to generalized functions, although their growth rates tend to the constant limit of 0.21.

Aside from being more realistic than the infinite plane-periodic geometry considered before, the spherical geometry considered here is of particular interest, in view of the Bondi-Gold theorem noted above, stating that the field in the insulators inside and outside the spherical shell cannot be amplified on the fast time scale. This result is again readily understood in terms of frozen flux: By the frozen flux theorem, field lines will remain with the fluid. But by continuity, fluid on the inner and outer surfaces of the shell will remain there. Therefore, one cannot change the number of field lines penetrating these surfaces, at least not on the fast advective time scale, only on the slow diffusive time scale on which the frozen flux theorem does not apply.

We have, however, demonstrated that these eigensolutions above do grow on the fast time scale. To be consistent with the Bondi-Gold theorem then, their structure must presumably be such that they have essentially no field lines penetrating the inner and outer surfaces.

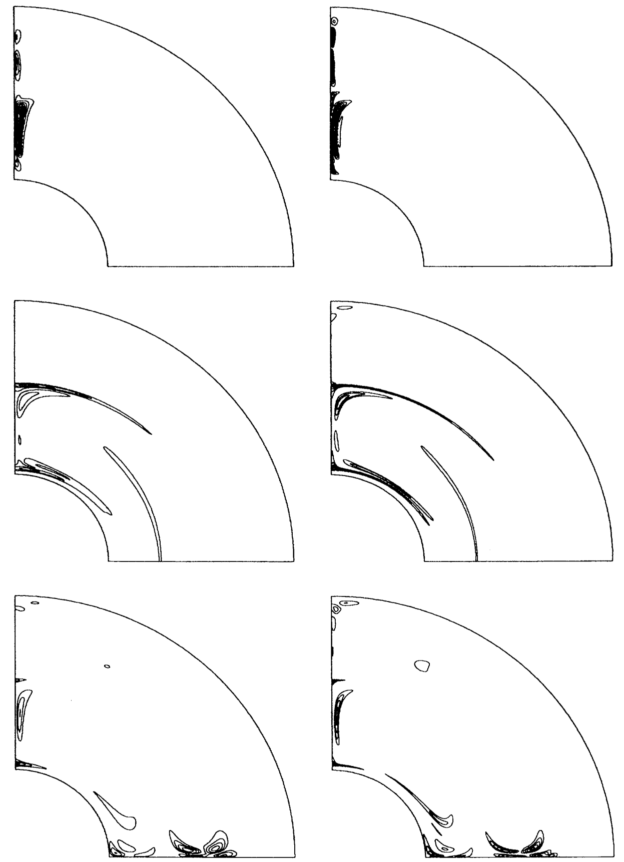

FIG. 3. The structure of the field in the particular meridional plane for which $\int B_\phi \, dS = 0$. $R_m = 10\,000$ on the left, 40 000 on the right. From top to bottom contours focus on the dominant structures. The truncations used for the $R_m = 10\,000$ and 40 000 runs were, respectively, 256×500 and 512×1000. As fine as they are, these structures are thus adequately resolved.

That this statement is qualitatively true is already apparent in Fig. 3, which slows that B_r is essentially zero on these surfaces. More quantitatively, consider the "pole strength" $H_{r'} \equiv \int_{r=r'} |B_r| \, dS$, the quantity identified by the theorem as being fixed in the limit $R_m \to \infty$. If we normalize the field such that the magnetic energy $\frac{1}{2} \int |\mathbf{B}|^2 \, dV = 1$, then the inner pole strength H_{r_i} is 0.023 for $R_m = 10\,000$, 0.019 for 20 000, and 0.014 for 40 000. The outer pole strengths H_{r_o} are even smaller. As R_m tends to infinity, the pole strengths thus tend to zero.

It is in this way that the Bondi-Gold theorem is met for the case at hand. At any finite R_m, where the theorem does not apply rigorously, the eigensolutions do have a small, finite pole strength, which also grows on the fast time scale. However, as R_m increases, this pole strength decreases, so that at infinite R_m, where the theorem does apply rigorously, the pole strength is zero. The field is then completely contained within the spherical shell and can thus grow on the fast time scale without violating the Bondi-Gold theorem.

The ideas developed in this work are the result of a series of discussions at the Isaac Newton Institute for Mathematical Sciences, Cambridge. We thank the Isaac Newton Institute for bringing us together and making these discussions possible. The calculations described here were done on the LANL Advanced Computing Laboratory's Cray T3D. The use of these resources is gratefully acknowledged.

[1] H. K. Moffatt, *Magnetic Field Generation in Electrically Conducting Fluids* (Cambridge University Press, Cambridge, England, 1978).
[2] E. N. Parker, *Cosmical Magnetic Fields: their Origin and their Activity* (Clarendon, Oxford, 1979).
[3] Ya. B. Zeldovich, A. A. Ruzmaikin, and D. D. Sokoloff, *Magnetic Fields in Astrophysics* (Gordon and Breach, New York, 1983).
[4] S. I. Vainshtein and Ya. B. Zeldovich, Sov. Phys. Usp. **15**, 159 (1972).
[5] H. K. Moffatt, Nature (London) **341**, 285 (1989).
[6] D. J. Galloway and M. R. E. Proctor, Nature (London) **356**, 691 (1992).
[7] H. Bondi and T. Gold, Mon. Not. R. Astron. Soc. **110**, 607 (1950).
[8] J. M. Finn and E. Ott, Phys. Fluids **31**, 2992 (1988).
[9] M. M. Vishik, Geophys. Astrophys. Fluid Dyn. **48**, 151 (1989).
[10] B. J. Bayly and S. Childress, Phys. Rev. Lett. **59**, 1573 (1987).
[11] A. D. Gilbert and S. Childress, Phys. Rev. Lett. **65**, 2133 (1990).
[12] A. D. Gilbert, Geophys. Astrophys. Fluid Dyn. **44**, 214 (1988).
[13] A. M. Soward, J. Fluid Mech. **180**, 267 (1987).
[14] A. D. Gilbert, Nature (London) **350**, 483 (1991).
[15] I. Klapper, J. Fluid Mech. **239**, 359 (1992).
[16] T. G. Cowling, Mon. Not. R. Astron. Soc. **94**, 39 (1934).
[17] H. K. Moffatt and M. R. E. Proctor, J. Fluid Mech. **154**, 493 (1985).
[18] R. Hollerbach, Phys. Fluids **6**, 2540 (1994).
[19] D. J. Galloway and M. R. E. Proctor (unpublished).